coatings

MDPI

Article

The Properties of the $CH_3NH_3PbI_3/TiO_2$ Composite Layer Prepared from PbO-TiO_2 Mesoporous Layer under Air Ambience

Qinmiao Chen [1,*], Wei Zhu [1], Yi Ni [1] and Hongcun Yuan [2]

[1] School of Physics, East China University of Science and Technology, 130 Meilong Road, Shanghai 200237, China
[2] School of Electrical and Information Engineering, Changzhou Institute of Technology, 229 South Tongjiang Road, Changzhou 213002, China
* Correspondence: jamechern@gmail.com

Abstract: In TiO_2-based perovskite solar cells (PSC), the preparation of the $CH_3NH_3PbI_3/TiO_2$ composite layer is very important, since the morphology of the perovskite adsorbed onto the surface of the TiO_2 nanoparticles has decisive significance for the absorption of the incident sunlight and separation of the generated carrier. The traditional two-step spin-coating method for the deposition of $CH_3NH_3PbI_3$ into the porous mesoporous TiO_2 layer usually suffers from filling block problems. In this study, the PbO-TiO_2 mesoporous layer was prepared with various ratios of Pb:Ti in the raw materials. Morphological, optical, and element analysis of the prepared thin films indicated that Pb was gradually mixed into the TiO_2 mesoporous layer with the increased Pb:Ti ratios. The element distribution characteristics of the optimal thin films showed that the distribution of Pb was uniform throughout the whole TiO_2 thin film, which indicates the successful mixing of Pb into the TiO_2 electrode layer. Combined with dip coating, the PbO-TiO_2 mesoporous layer was prepared into a $CH_3NH_3PbI_3/TiO_2$ composite layer and subsequently to a solar cell device. The prepared solar cell shows a short-circuit photocurrent density of 16.4 mA/cm^2, an open-circuit voltage of 900 mV, a fill factor of 61%, and a power conversion efficiency (PCE) of 9.00%. The PCE of the PSC is promoted by nearly 25% when compared with that prepared with the traditional method. The proposed preparation method that combines TiO_2 nanoparticle electrode with a mixing and dip coating provides a new effective way to improve the deposition of perovskite into the mesoporous TiO_2 layer, which is very helpful for the fabrication of high-efficiency and low-cost PSC.

Keywords: perovskite absorption layer; PbO-TiO_2 mesoporous layer; $CH_3NH_3PbI_3/TiO_2$ composite layer; photoelectric properties

check for updates

Citation: Chen, Q.; Zhu, W.; Ni, Y.; Yuan, H. The Properties of the $CH_3NH_3PbI_3/TiO_2$ Composite Layer Prepared from PbO-TiO_2 Mesoporous Layer under Air Ambience. *Coatings* **2023**, *13*, 669. https://doi.org/10.3390/coatings13040669

Academic Editor: Alessandro Latini

Received: 1 February 2023
Revised: 16 March 2023
Accepted: 20 March 2023
Published: 24 March 2023

Copyright: © 2023 by the authors. Licensee MDPI, Basel, Switzerland. This article is an open access article distributed under the terms and conditions of the Creative Commons Attribution (CC BY) license (https://creativecommons.org/licenses/by/4.0/).

1. Introduction

The perovskite solar cell [1], with material properties and a preparation process similar to traditional dye-sensitized and compound thin film solar cells (such as $CuIn_xGa_{1-x}(S,Se)_2$, $Cu_2ZnSn(S,Se)_4$) [2], has attracted much attention and made great progress in recent years. Perovskite materials have very important excellent properties, such as: (1) Strong optical absorption. The energy band gap value of perovskite is about 1.5 eV, which can absorb almost all visible light for photoelectric conversion [3]. (2) Good carrier transport characteristic. Perovskite has unique bipolar carrier transport properties [1], which can transport electrons and holes generated by absorption of the incident sunlight at the same time, and the carrier diffusion length can reach 1 μm [4]. (3) Low preparation conditions and cost. Perovskite and other functional thin films included in the solar cells can be prepared using a solution route at low temperatures and a low cost. The excellent properties of perovskite coupled with its compatibility with low-cost preparation technologies result in extremely rapid developments of perovskite solar cells. In 2009, the efficiency of perovskite

solar cells was only 3.8% [5], but at present its efficiency has reached 25.7% [6,7]. It can be said that perovskite solar cells are one of the most outstanding solar cells with a high efficiency and low costs.

The perovskite absorption layer is usually deposited into the TiO_2 porous mesoporous layer to fabricate solar cells with good properties. Under sunlight, the carriers generated in the solar cell are determined by the perovskite absorption layer and are subsequently separated at the interface of the perovskite and TiO_2 thin films, so the morphology of the deposited perovskite absorption layer is significant for the properties of the prepared solar cells [8–13]. At present, the perovskite thin film is mostly prepared by a two-step spin-coating method [14,15]. The perovskite is expected to be deposited into the pores of the entire electrode transport layer during the fabrication process [13,16,17]. However, it usually suffers from filling block problems. The bottom side of the electrode transport layer usually cannot be filled by the perovskite and therefore leaves gaps. This could result in a reduction in the absorption of incident sunlight and, moreover, an increase in carrier recombinations at the gaps [9]. Han H. group also reported the perovskite filling problem in perovskite solar cells [18]. The researchers changed the traditional perovskite raw material CH_3NH_3I to $HOOC(CH_2)_4NH_3I$, and filled the perovskite material with a one-step spin-coating method. The results showed that the perovskite prepared by $HOOC(CH_2)_4NH_3I$ has a better filling into the TiO_2 electrode than that prepared traditionally by $CH_3NH_3PbI_3$. In addition, the perovskite filling rate of the prepared solar cell is also much higher. Therefore, perovskite filling of the porous TiO_2 electrode could be extremely important for the fabrication of high-efficiency perovskite solar cells. Additionally, in order to prepare high-efficiency solar cells, some researchers designed the electrode transport layer as a nanorod array to increase the filling amount of perovskite [8,9,19]. However, it is difficult to prepare the nanorod array electrode with good morphology and stability. The upper side of the prepared nanorod array electrode is often staggered, which hinders the filling of perovskite into the bottom side.

Different from the nanorod array electrode, the mesoporous electrode is composed of nanoparticles, which are distributed uniformly and are closely arranged in the electrode. The formed pore space between the nanoparticles is therefore controllable and stable, which is conducive to the deposition and morphological control of the perovskite. TiO_2 nanoparticle electrodes are classically used as an electron transport in dye-sensitized solar cells, and its preparation method is mature and simple. At present, TiO_2 nanoparticle electrodes have also been widely employed as the electron transport layer for perovskite solar cells [3,5,10–13]. TiO_2 nanoparticle electrodes play the same role in dye-sensitized solar cells and in perovskite solar cells. They serve as both the skeleton for the absorption layer deposition and the transport path of the generated carrier. However, when the popular spin-coating method is used, the filling of absorption materials in perovskite solar cells is not as good as that in dye-sensitized solar cells. In the dye-sensitized solar cell, the filling process of the dye does not include chemical reactions. As the dye is used in the formation of a solution, it can be fully adsorbed onto the whole TiO_2 nanoparticle electrode with a good uniformity. However, in the perovskite solar cell (such as $CH_3NH_3PbI_3$), the deposition of perovskite into the TiO_2 nanoparticle electrodes often includes the chemical reaction of PbI_2 and CH_3NH_3I. In the deposition process, PbI_2 is infiltrated first, then the CH_3NH_3I is infiltrated. Subsequently, CH_3NH_3I reacts with PbI_2 to generate the perovskite $CH_3NH_3PbI_3$. However, the solubility of PbI_2 is not so good, so it is not easy to infiltrate the bottom of the TiO_2 nanoparticle electrode using the spin-coating method. Furthermore, CH_3NH_3I will react fast with PbI_2 to form solid perovskite $CH_3NH_3PbI_3$ at the upper side of the electrode when CH_3NH_3I is deposited onto the PbI_2-included TiO_2 nanoparticle electrode by spin-coating [12]. As a result, the formation of solid perovskite in the upper side of the electrode hinders the further filling of perovskite into the bottom side. This is not good for the fabrication of high-efficiency and low-cost solar cells [20].

In this study, based on the formation mechanism of a perovskite absorption layer, a facile and efficient fabrication route combining TiO_2 nanoparticle electrodes with a mixing

and dip coating was proposed, to improve the deposition of perovskite into the TiO_2 nanoparticle electrode. The morphological, optical, and crystal structure and photoelectric conversion properties of the prepared thin films were studied using scanning electron microscopy equipped with an X-ray energy dispersive spectrometer, a UV-vis-NIR spectrophotometer, a power X-ray diffraction, and an I-V test system, respectively.

2. Experiment

2.1. Preparation of Precursor Solution

The materials used in this study were purchased from commercial sources without further purification. The TiO_2 solution was prepared by diluting commercial TiO_2 slurry in ethanol. Under stirring at 70 °C, 0.461 g PbI_2 (99.99%) was dissolved in 1 mL N,N-dimethylformamide (DMF) to prepare PbI_2 solution. A CH_3NH_3I solution of 10 mg/mL was prepared by dissolving CH_3NH_3I in isopropyl alcohol (IPA). To prepare the hole transport layer (HTL), 72.3 mg 2,2′,7,7′-tetrakis(N,N-di-p-methoxypheny-amine)-9,9′-spirobifluorene (spiro-OMeTAD), 28.8 µL ter-butylpyridine (TBP), 17.5 µL of pre-prepared solution from 52 mg lithium bis(trifluoromethanesulfonyl)imide (Li-TFSI) in 100 µL acetonitrile, and 1 mL chlorobenzene were mixed. The main materials used in this study are also listed in Table 1 below.

Table 1. The list of main materials used in this study.

Name	PbI_2	N,N-Dimethyl formamide	CH_3NH_3I	2,2′,7,7′-Tetrakis(N,N-Di-P-Methoxypheny-Amine)-9,9′-Spirobifluorene	Isopropyl Alcohol	Ter-butylpyridine	Lithium bis(trifluoromethanesulfonyl)imide	Acetonitrile	Chlorobenzene
Purity	99.99%	99.9%	99.5%	99.8%	99.9%	96%	98%	-	99.5%
Amount/ Concentration	0.461 g	1 mL	500 mg	72.3 mg	50 mL	28.8 µL	52 mg	100 µL	1 mL

2.2. Preparation of Pb-TiO_2 Electrode, $CH_3NH_3PbI_3/TiO_2$ Composite Layer, and Perovskite Solar Cell

When compared to the traditional methods, the main difference in the proposed method lies in the preparation of the perovskite absorption layer. Figure 1 shows the preparation diagram of the perovskite solar cell using the proposed method. The fluorine-doped tin oxide (FTO) glass was first etched by machining and was then cleaned by a standard process. The TiO_2 was deposited by spin-coating in accordance with previously published articles [21,22]. First, a compact TiO_2 (c-TiO_2) layer was spin-coated at 5000 rpm for 30 s and was then annealed at 500 °C for 30 min. A mesoporous TiO_2 (m-TiO_2) layer with various PbO powder (99.99%) mixings (Pb:Ti was set at mole ratio of 1:10, 1:8, 1:6, 1:4, 1:2, and 1:1) was then deposited onto the c-TiO_2/FTO glass by spin-coating at 3000 rpm for 30 s. After that, the prepared sample was annealed at 500 °C for 30 min again. The annealing process is a key step in the preparation of a TiO_2 electrode, which directly affects the crystallinity, morphology, adsorption, adhesion, and element mixing of the prepared electrode, and further affects the adsorption of the perovskite absorption layer, the lifetime of electrons in the TiO_2 nanoparticle electrode, the interface carrier separation/recombination, and the effect of elemental mixing. Then, the prepared and annealed PbO-TiO_2 nanoparticle electrode was immersed in a hydriodic acid (HI) solution (55% in water) to convert PbO into PbI_2. After drying at 125 °C, the PbI_2/m-TiO_2/c-TiO_2/FTO glass sample was immersed in a CH_3NH_3I solution with isopropyl alcohol for 20 s to prepare $CH_3NH_3PbI_3$/m-TiO_2/c-TiO_2/FTO glass. The prepared sample was rinsed with an IPA solution and was then annealed at 70 °C for 5 min on a hot plate for the subsequent deposition of HTL and Au, and finally the solar cell device.

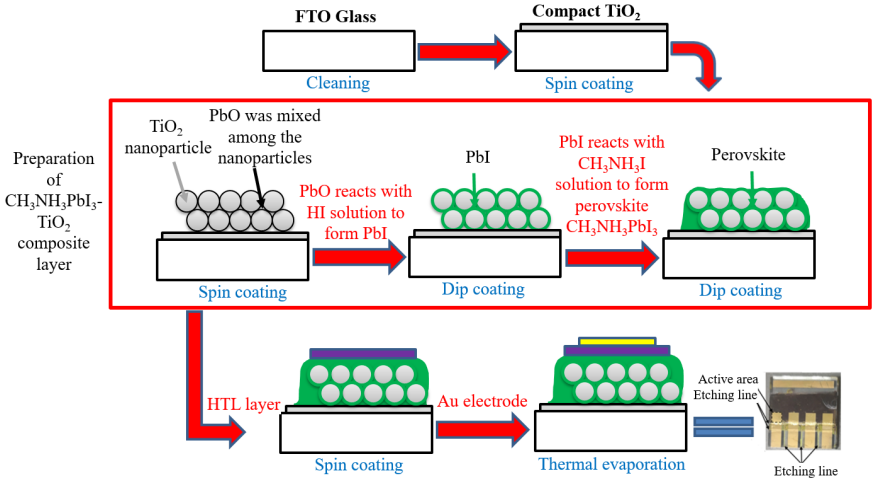


Figure 1. The preparation diagram for the PbO-TiO_2 mesoporous layer, $CH_3NH_3PbI_3$/TiO_2 composite layer, and solar cell.

For a traditional two-step spin-coating method, the PbI_2 layer was deposited onto the m-TiO_2 layer by spin-coating at 2000 rpm for 5 s and 5000 rpm for 20 s. Then, the sample underwent the annealing process at 70 °C for 10 min. After cooling down to room temperature, the CH_3NH_3I solution was spin-coated onto the sample at 3000 rpm for 5 s and 5000 rpm for 20 s to form $CH_3NH_3PbI_3$/m-TiO_2/c-TiO_2/FTO glass. The prepared sample was also rinsed with an IPA solution and was then annealed at 70 °C for 5 min on a hot plate.

After that, for both samples prepared by the proposed and traditional methods, the HTL was spin-coated onto the annealed $CH_3NH_3PbI_3$/m-TiO_2/c-TiO_2/FTO glass at 5000 rpm for 30 s. All these steps were conducted in ambient air. Finally, Au back contact (0.33 cm × 0.33 cm) was thermally evaporated onto the top of the HTL/$CH_3NH_3PbI_3$/m-TiO_2/c-TiO_2/FTO glass to finish the fabrication of the perovskite solar cell.

2.3. Characterization

Scanning electron microscopy (SEM, S-3400N, JEOL, Tokyo, Japan) equipped with an X-ray energy dispersive spectrometer (EDS, JEOL, Tokyo, Japan) was employed to analyze the surface morphology and structure of the prepared samples. Power X-ray diffraction (XRD, 18KW/D/MAX 2550 VB, RIGAKU, Tokyo, Japan; Cu Kα radiation) was used to study the crystalline property of the samples. The ultraviolet-visible (UV-vis) absorbance spectra of the prepared samples were measured with a UV-vis-NIR spectrophotometer (Lambda 950, Varian, Perkinelmer, MA, USA). The photocurrent density-voltage (J-V) property of the fabricated solar cell devices was obtained with a keithley model 2400 digital source meter and a solar simulator (Oriel Sol3A, Newport, State of California, USA), which was calibrated to AM 1.5, 100 $mW \cdot cm^{-2}$ by a standard silicon photodiode before the J-V test.

3. Results and Discussion

3.1. The Effect of Pb:Ti on the Properties of Prepared PbO-TiO_2 Composite Thin Films

The top view and optical properties of the thin films prepared from a PbO-TiO_2 mixture, as mentioned in Section 2.2, were studied. Figure 2a shows the top view of TiO_2 thin films prepared with different ratios of Pb:Ti. The color of the PdO-TiO_2 nanoparticle electrode slowly changed to yellow as the Pb content increased, which indicates the gradual mixing of Pb into the TiO_2 nanoparticle electrode. However, when the mixing of Pb reaches 1:1 of Pb:Ti, the prepared nanoparticle electrode seems loose and is easily peeled off from the substrate, as can be seen from the sample in the lower right corner of the 1:1 picture in Figure 2a. Therefore, the mole ratio of 1:1 for Pb:Ti was not suitable for the fabrication of solar cells and was not chosen for the subsequent experiments. Figure 2b shows the repre-

sentative TiO_2/PbI_2 thin film prepared by dipping the PbO-TiO_2 nanoparticle electrode with Pb:Ti of 1:2 into the HI solution. The thin film changed to golden yellow, with the PbO transforming to PbI_2. Figure 2c shows the top-view picture of the $CH_3NH_3PbI_3/TiO_2$ thin film by dipping the PbI_2/TiO_2 thin film into a CH_3NH_3I solution. As can be seen from the figure, the color of the sample has obviously changed to black, indicating the successful formation of $CH_3NH_3PbI_3$ compounds.

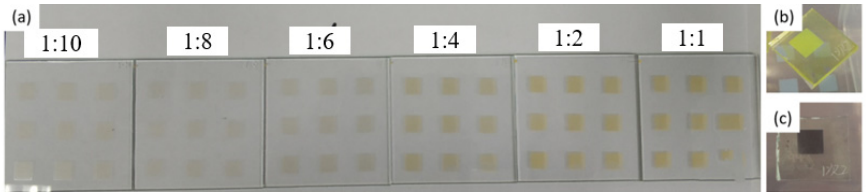


Figure 2. The top-view pictures of (**a**) the TiO_2 thin film prepared from different ratios of Pb:Ti; (**b**) the PbI_2/TiO_2 thin film prepared by dipping the PbO-TiO_2 nanoparticle electrode into HI solution; (**c**) the perovskite/TiO_2 thin film prepared by dipping the PbI_2/TiO_2 thin film into CH_3NH_3I solution.

Figure 3 shows the optical absorption characteristics of the $CH_3NH_3PbI_3/TiO_2$ composite thin films prepared from the PbO-TiO_2 with Pb:Ti ratios of 1:10, 1:8, 1:6, 1:4, and 1:2 in the raw materials (sample with Pb:Ti ratio of 1:1 was not measured since it is not suitable to fabricate solar cells as mentioned above; sample prepared by the proposed method with no Pb mixed with TiO_2 (sample 0), and another sample prepared by the traditional two-step spin-coating method were also included). As can be seen from the figure, the absorption of the samples was enhanced by Pb mixing, indicating that the $CH_3NH_3PbI_3$ compound was successfully formatted in the composite thin film. Comparing the UV-vis absorption of the prepared $CH_3NH_3PbI_3/TiO_2$ composite thin films with different ratios of Pb:Ti, the absorption of the samples generally becomes stronger with an increasing ratio of Pb:Ti, and it reached the top in the visible spectrum range when Pb:Ti was 1:2. The EDS analysis confirmed that the content of Pb in the $CH_3NH_3PbI_3/TiO_2$ thin films increases with the increasing ratio of Pb:Ti in the raw material, as shown in Table 2. The Pb:Ti reached 0.388 in the prepared $CH_3NH_3PbI_3/TiO_2$ composite thin films when the ratio of Pb:Ti was set to 1:2 in the raw materials, as shown in Tables 2 and 3. As can be seen from the figure, the absorbance of the $CH_3NH_3PbI_3/TiO_2$ composite thin films prepared by the proposed method with Pb:Ti of 1:2 is stronger at the visible spectrum range when compared with that prepared by the traditional method. This could be due to the increase in perovskite being filled into the TiO_2 electrode using the proposed method than that prepared by the traditional method. Therefore, Pb:Ti with a ratio of 1:2 was chosen for the following study.

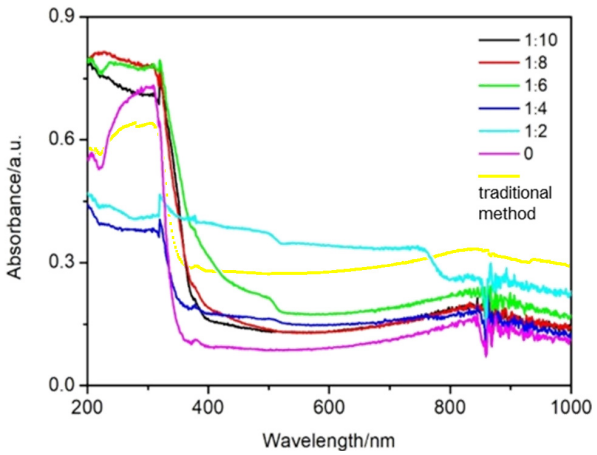


Figure 3. UV-vis absorbance spectrum of the $CH_3NH_3PbI_3/TiO_2$ composite thin films prepared from PbO-TiO_2 thin film with different ratios of Pb:Ti.

Table 2. EDS analysis of the $CH_3NH_3PbI_3/TiO_2$ composite thin films prepared from PbO-TiO_2 thin film with different ratios of Pb:Ti.

Pb:Ti	EDS Result
1:10	0.037
1:08	0.1
1:06	0.097
1:04	0.125
1:02	0.388

Table 3. The weight (%) and atomic (%) for each element in the sample with Pb:Ti of 1:2.

Element	Wt%	At%
CK	02.27	07.01
OK	23.93	55.57
NaK	01.78	02.88
MgK	00.45	00.69
SiK	05.09	06.73
PbM	41.17	07.38
CaK	00.77	00.72
TiK	24.53	19.02

The elemental distributions of Pb and Ti in the $CH_3NH_3PbI_3/TiO_2$ composite thin film prepared from Pb:Ti of 1:2 are given in Figure 4. Figure 4a shows the measured field of the sample. According to Figure 4b–d, the distribution of Pb and Ti is very uniform throughout the whole thin film, which demonstrates that perovskite was uniformly filled into the TiO_2 nanoparticle electrode. Perovskite solar cells prepared by the traditional two-step spin-coating method often suffer from the inadequate filling of perovskite at the bottom side of the electrode, which not only reduces the absorption of the incoming sunlight but also increases the recombination of carriers at the gaps [9,18,20]. Therefore, the uniform adsorption of perovskite onto the surface of TiO_2 nanoparticles through the whole electrode is quite important, and would improve the performance of the solar cells. In addition, the atom ratio of Pb and I in the prepared $CH_3NH_3PbI_3/TiO_2$ composite thin film was also estimated by the EDS to be 1:2.58, which is between 1:3 of $CH_3NH_3PbI_3$ and 1:2 of PbI_2.

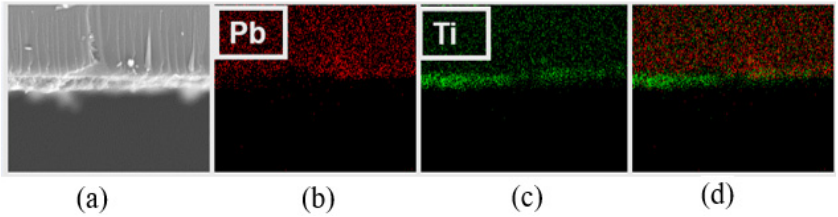


Figure 4. EDS images of Pb and Ti in the $CH_3NH_3PbI_3/TiO_2$ composite thin film prepared from Pb:Ti of 1:2. (**a**) characterization region; (**b**) Pb; (**c**) Ti; (**d**) Pb and Ti.

3.2. Optimization of Dip Coating for the Preparation of Perovskite Absorption Layer

The prepared $CH_3NH_3PbI_3/TiO_2$ composite thin film was studied using XRD, and the result is shown in Figure 5. The 1ci-$MAPbI_3/TiO_2$ sample is obtained by dipping the PbI_2/TiO_2 thin film into a CH_3NH_3I (for the convenience of picture display, it is expressed as MAI, the same goes for below) solution once, the 2ci-$MAPbI_3/TiO_2$ sample is obtained by dipping the PbI_2/TiO_2 thin film into the MAI solution twice, while 10 days $MAPbI_3/TiO_2$ sample stands the 2ci-$MAPbI_3/TiO_2$ sample after placing it for 10 days to observe the change in the perovskite crystal phase. As can be seen from the XRD pattern, TiO_2 has a main peak at 25.3°, which belongs to the 101 crystal phase (PCPDF #21-1272). For PbO, the peaks at 22.1°, 32.4°, 39.6°, 46.2°, and 57.3° correspond to the 110, 200, 121, 030, and 230 crystal phases (PCPDF #38-1477), respectively. As for PbI_2, the peaks at 12.6°, 25.7°,

34.0°, 39.5°, 45.2°, 52.3°, 68.4°, and 73.2°correspond to the 001, 002, 102, 110, 101, 004, 212, and 301 crystal phases (PCPDF #07-0235), respectively. The peaks at 14.2°, 28.5°, and 31.9°correspond to the 110, 220, and 310 crystal phases of $MAPbI_3$, respectively, which demonstrate the successful formation of tetrahedral perovskite [12,23–25]. However, the prepared perovskite thin film still contains a PbI_2 phase at 12.6°, indicating that PbI_2 may exist in the prepared composite thin film (consistent with the EDS discussion above). There is also a PbO phase at 22.6° and 39.6°, which may come from the oxidization of PbI_2 into the open-air ambience. In the prepared composite thin film, there also exists a crystal phase that is difficult to identify. Compared with the one-dipping process, the sample prepared by dipping twice shows better crystallinity, which indicates that more perovskite could be obtained from the sample. The full width at half maxima (FWHM) of the $MAPbI_3$ phases 110, 220, and 310 are about 0.07°, 0.19°, and 0.89°, respectively, as shown in Table 4. The FWHM of the $MAPbI_3$ crystal phases 110 and 220 are small, while the FWHM of crystal phase 310 is a bit big, which indicates that the crystallinity of $MAPbI_3$ can be further improved in the future. As can be seen from the figure, the prepared perovskite is also stable after 10 days, although the diffraction peak intensity is slightly weakened.

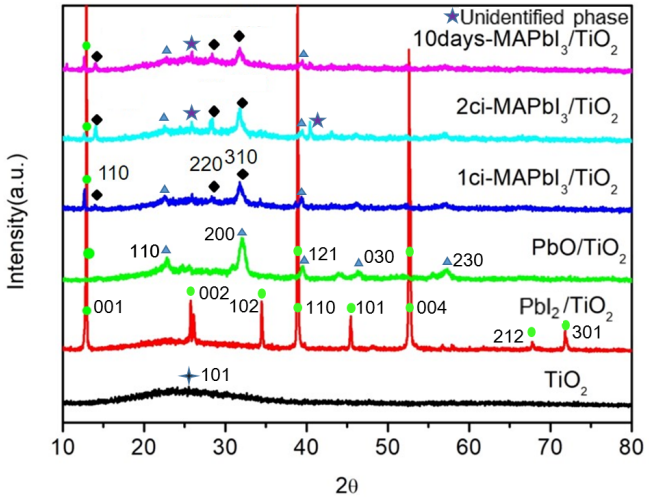
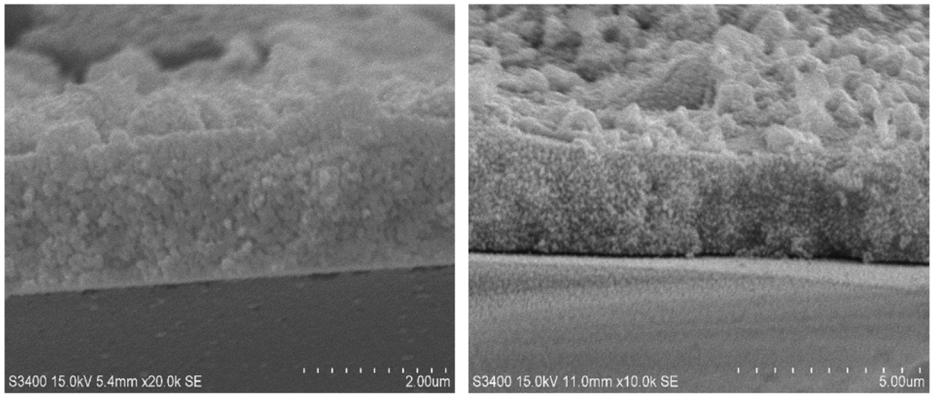


Figure 5. XRD diffraction patterns of the prepared $CH_3NH_3PbI_3/TiO_2$ composite thin film.

Table 4. The FWHM of $MAPbI_3$ phases 110, 220, and 310.

Crystal Phase	FWHM/°
110	0.07
220	0.19
310	0.89

The SEM morphology of the $CH_3NH_3PbI_3/TiO_2$ composite thin film prepared by the proposed method with dipping twice was compared with that prepared by the traditional two-step spin-coating method, as shown in Figure 6. As can be seen from the filling of pores in the TiO_2 nanoparticle electrode, the sample prepared with the proposed method is more compact than that prepared by the traditional method. It is shown that the proposed method is helpful for the deposition of perovskite into the TiO_2 nanoparticle electrode throughout the whole electrode, which would increase the absorption of incident light and reduce carrier recombination [12,26,27]. In addition, as can be observed from the sample, the interface between the composite thin film and the substrate prepared by the proposed method is also more closely connected than that prepared by the traditional two-step spin-coating method. This is helpful for the smooth extraction of electrons outside of the $CH_3NH_3PbI_3/TiO_2$ composite layer, and therefore further reduces carrier recombination.



(a) (b)

Figure 6. SEM morphology of the $CH_3NH_3PbI_3/TiO_2$ composite thin film (**a**) prepared by the proposed method; (**b**) by the traditional two-step spin-coating method.

The above sample was fabricated into solar cells by sequential deposition of the HTL and Au electrode. The J-V results of the $CH_3NH_3PbI_3/TiO_2$ composite thin film prepared by the proposed method and the traditional two-step spin-coating method were compared, as shown in Figure 7. The black curve in the figure is the photoelectric conversion characteristic of the solar cell prepared by the proposed method and the red one in the figure is the solar cell prepared by the traditional two-step spin-coating method. The slight irregularities in the J-V curves may come from the uneven interfaces between the prepared solar cell thin films. The power conversion efficiency (PCE) of the solar cell prepared by the proposed method is 9% with a short-circuit photocurrent density (J_{SC}) of 16.4 mA/cm^2, an open-circuit voltage (V_{OC}) of 0.90 V, and a fill factor (FF) of 61%. Meanwhile, the PCE of the solar cell prepared by the traditional two-step spin-coating method is 7.2% with a J_{SC} of 14.1 mA/cm^2, a V_{OC} of 0.88 V, and an FF of 58%. The PCE of the solar cell prepared by the proposed method is about 25% higher than that prepared by the traditional two-step spin-coating method. The improved conversion efficiency is mainly due to the increase inJ_{sc} from 14.1 mA/cm^2 to 16.4 mA/cm^2, which may be caused by more perovskite being filled into the TiO_2 nanoparticle by the proposed method, increasing the absorption of the incident light, and therefore generating more carriers. The increased filling of perovskite into the bottom of the TiO_2 nanoparticle electrode can also improve the V_{oc} of the solar cell, since it avoids the recombination of electrons and holes at the gaps that usually appear in the bottom side of the $CH_3NH_3PbIs_3/TiO_2$ composite thin film fabricated by the traditional two-step spin-coating method [18]. In this study, the thickness of the $CH_3NH_3PbI_3/TiO_2$ composite thin film prepared by the proposed method is similar to that prepared by the traditional two-step spin-coating method, which is around 2.2 μm. The thickness of the $CH_3NH_3PbI_3/TiO_2$ composite thin film is bigger than that in a high-efficiency perovskite solar cell, whose thickness is around 850 nm (which also can be increased to 1150 nm for easy fabrication [28]). The present PCE of the prepared solar cell is not so high, which may be due to the excessively thick $CH_3NH_3PbI_3/TiO_2$ composite thin film that results in more carrier recombinations [28,29]. Next, the fabrication process for the PSC will be further optimized to promote the performance of the solar cell.

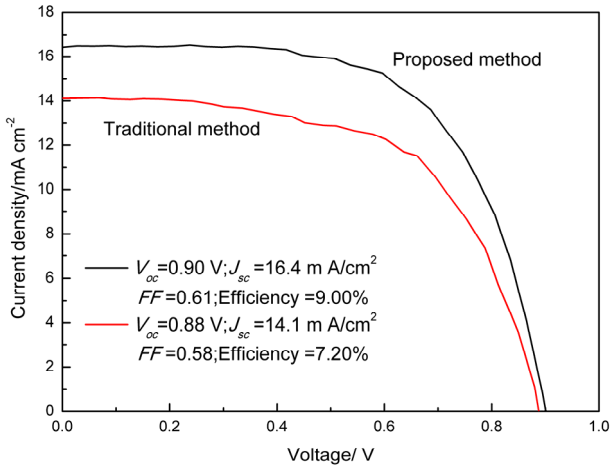


Figure 7. J-V curve of the $CH_3NH_3PbI_3/TiO_2$ composite thin film prepared with the proposed method and the traditional two-step spin-coating method.

4. Conclusions

In this study, a facile fabrication method to improve the perovskite deposition into the TiO_2 nanoparticle electrode was proposed, and it has proven to be effective. It has been shown that Pb can be successfully mixed into the TiO_2 nanoparticle electrode and its content increases with the Pb:T ratio that is increased in the raw materials. The effect of Pb:Ti on the properties of the prepared PbO-TiO_2 thin film was optimized. The atom ratio of Pb and I was estimated to be 1:2.58 in the perovskite absorption layer prepared from Pb:Ti of 1:2. The prepared perovskite/TiO_2 composite thin film has a uniform Pb/Ti elemental distribution, and its optical absorption is also excellent. The obtained perovskite/TiO_2 composite thin film shows the 110, 220, and 310 crystal phases at 14.2°, 28.5°, and 31.9°, demonstrating the formation of tetrahedral perovskite. Moreover, the sample prepared with dipping twice shows more compact morphology and better crystallinity (especially at crystal phases 110 and 310). The morphology and crystallinity of the prepared perovskite improve the short-circuit photocurrent density and open-circuit voltage of the fabricated solar cell when compared to that prepared by the traditional two-step spin-coating method. The PCE of the solar cell prepared by the proposed method is 9% (J_{SC} of 16.4 mA/cm^2, V_{OC} of 0.90 V, and FF of 61%), about 25% higher than that prepared by the traditional two-step spin-coating method. This could be due to more perovskite that is filled into the TiO_2 nanoparticle in the proposed method, which not only increases the absorption of incident light and therefore can generate more carriers, but also reduces the carrier recombination in the prepared perovskite/TiO_2 composite thin film. The proposed method also has an important value for the fabrication of other relative photoelectric functional thin films or devices.

Author Contributions: Conceptualization, Q.C. and H.Y.; methodology, W.Z. and Y.N.; formal analysis, Y.N. and Q.C.; investigation, Q.C., Y.N. and H.Y.; writing—original draft preparation, Q.C.; writing—review and editing, Y.N. and H.Y.; project administration, Q.C.; funding acquisition, Q.C. All authors have read and agreed to the published version of the manuscript.

Funding: This research was funded by the National Natural Science Foundation of China, grant number 11604097 and the East China University of Science and Technology, grant number YK0142119.

Institutional Review Board Statement: Not applicable.

Informed Consent Statement: Not applicable.

Data Availability Statement: Not applicable.

Conflicts of Interest: The authors declare no conflict of interest.

References

1. Lee, M.M.; Teuscher, J.; Miyasaka, T.; Murakami, T.N.; Snaith, H.J. Efficient hybrid solar cells based on meso-superstructured organometal halide perovskites. *Science* **2012**, *338*, 643–647. [CrossRef]
2. Lee, T.D.; Ebong, A.U. A review of thin film solar cell technologies and challenges. *Renew. Sustain. Energy Rev.* **2017**, *70*, 1286–1297. [CrossRef]
3. Rhee, J.H.; Chung, C.C.; Diau, E.W.G. A perspective of mesoscopic solar cells based on metal chalcogenide quantum dots and organometal-halide perovskites. *NPG Asia Mater.* **2013**, *5*, e68. [CrossRef]
4. Stranks, S.D.; Eperon, G.E.; Grancini, G.; Menelaou, C.; Alcocer, M.J.P.; Leijtens, T.; Herz, L.M.; Petrozza, A.; Snaith, H.J. Electron-hole diffusion lengths exceeding 1 micrometer in an organometal trihalide perovskite absorber. *Science* **2013**, *342*, 341–344. [CrossRef] [PubMed]
5. Kojima, A.; Teshima, K.; Shirai, Y.; Miyasaka, T. Organometal halide perovskites as visible-light sensitizers for photovoltaic cells. *J. Am. Chem. Soc.* **2009**, *131*, 6050–6051. [CrossRef] [PubMed]
6. Green, M.A.; Dunlop, E.D.; Siefer, G.; Yoshita, M.; Kopidakis, N.; Bothe, K.; Hao, X.J. Solar cell efficiency tables (Version 61). *Prog. Photovolt. Res. Appl.* **2023**, *31*, 3–16. [CrossRef]
7. Jeong, M.; Choi, I.W.; Go, E.M.; Cho, Y.J.; Kim, M.J.; Lee, B.K.; Jeong, S.H.; Jo, Y.H.; Choi, H.W.; Lee, J.Y.; et al. Stable perovskite solar cells with efficiency exceeding 24.8% and 0.3-V voltage loss. *Science* **2020**, *369*, 1615–1620. [CrossRef] [PubMed]
8. Kumar, M.H.; Yantara, N.; Dharani, S.; Graetzel, M.; Mhaisalkar, S.; Boix, P.P.; Mathews, N. Flexible, low-temperature, solution processed ZnO-based perovskite solid state solar cells. *Chem. Commun.* **2013**, *49*, 11089–11091. [CrossRef] [PubMed]
9. Kim, H.S.; Lee, J.W.; Yantara, N.; Boix, P.P.; Kulkarni, S.A.; Mhaisalkar, S.; Grätzel, M.; Park, N.-G. High efficiency solid-state sensitized solar cell-based on submicrometer rutile TiO_2 nanorod and $CH_3NH_3PbI_3$ perovskite sensitizer. *Nano Lett.* **2013**, *13*, 2412–2417. [CrossRef]
10. Bi, D.; Moon, S.J.; Häggman, L.; Boschloo, G.; Yang, L.; Johansson, E.M.J.; Nazeeruddin, M.K.; Grätzel, M.; Hagfeldt, A. Using a two-step deposition technique to prepare perovskite ($CH_3NH_3PbI_3$) for thin film solar cells based on ZrO_2 and TiO_2 mesostructures. *RSC Adv.* **2013**, *3*, 18762–18766. [CrossRef]
11. Zhao, Y.; Zhu, K. Charge transport and recombination in perovskite (CH_3NH_3)PbI_3 sensitized TiO_2 solar cells. *J. Phys. Chem. Lett.* **2013**, *4*, 2880–2884. [CrossRef]
12. Burschka, J.; Pellet, N.; Moon, S.J.; Humphry-Baker, R.; Gao, P.; Nazeeruddin, M.K.; Grätzel, M. Sequential deposition as a route to high-performance perovskite-sensitized solar cells. *Nature* **2013**, *499*, 316–319. [CrossRef] [PubMed]
13. Shi, J.; Luo, Y.; Wei, H.; Luo, J.; Dong, J.; Lv, S.; Xiao, J.; Xu, Y.; Zhu, L.; Xu, X. Modified Two-Step Deposition Method for High-Efficiency TiO_2/$CH_3NH_3PbI_3$ Heterojunction Solar Cells. *ACS Appl. Mater. Interfaces* **2014**, *6*, 9711–9718. [CrossRef] [PubMed]
14. Wu, J.; Xu, X.; Zhao, Y.; Shi, J.J.; Xu, Y.; Luo, Y.H.; Li, D.M.; Wu, H.J.; Meng, Q.B. DMF as an Additive in a Two-Step Spin-Coating Method for 20% Conversion Efficiency in Perovskite Solar Cells. *ACS Appl. Mater. Interfaces* **2017**, *9*, 26937–26947. [CrossRef]
15. Han, Y.; Xie, H.; Lim, E.L.; Bi, D. Review of Two-Step Method for Lead Halide Perovskite Solar Cells. *Solar RRL* **2022**, *6*, 2101007. [CrossRef]
16. Eperon, G.E.; Burlakov, V.M.; Docampo, P.; Goriely, A.; Snaith, H.J. Morphological Control for High Performance, Solution-Processed Planar Heterojunction Perovskite Solar Cells. *Adv. Funct. Mater.* **2014**, *24*, 151–157. [CrossRef]
17. Chen, Q.; Zhou, H.; Hong, Z.; Luo, S.; Duan, H.S.; Wang, H.H.; Liu, Y.; Li, G.; Yang, Y. Planar heterojunction perovskite solar cells via vapor-assisted solution process. *J. Am. Chem. Soc.* **2013**, *136*, 622–625. [CrossRef]
18. Mei, A.; Li, X.; Liu, L.; Ku, Z.; Liu, T.; Rong, Y.; Xu, M.; Hu, M.; Chen, J.; Yang, Y.; et al. A hole-conductor–free, fully printable mesoscopic perovskite solar cell with high stability. *Science* **2014**, *345*, 295–298. [CrossRef] [PubMed]
19. Jiang, Q. Rutile TiO_2 Nanowires Perovskite Solar Cells. *Chem. Commun.* **2014**, *50*, 14720–14723. [CrossRef] [PubMed]
20. Leijtens, T.; Lauber, B.; Eperon, G.E.; Stranks, S.D.; Snaith, H.J. The Importance of Perovskite Pore Filling in Organometal Mixed Halide Sensitized TiO_2-Based Solar Cells. *J. Phys. Chem. Lett.* **2014**, *5*, 1096–1102. [CrossRef] [PubMed]
21. Dastan, D.; Gosavi, S.W.; Chaure, N.B. Studies on Electrical Properties of Hybrid Polymeric Gate Dielectrics for Field Effect Transistors. *Macromol. Symp.* **2015**, *347*, 81–86. [CrossRef]
22. Dastan, D.; Londhe, P.U.; Chaure, N.B. Characterization of TiO_2 nanoparticles prepared using different surfactants by sol–gel method. *J. Mater. Sci. Mater. Electron.* **2014**, *25*, 3473–3479. [CrossRef]
23. Liu, M.; Johnston, M.B.; Snaith, H.J. Efficient planar heterojunction perovskite solar cells by vapour deposition. *Nature* **2013**, *501*, 395–398. [CrossRef] [PubMed]
24. Chen, Y.; Li, B.; Huang, W.; Gao, D.; Liang, Z. Efficient and reproducible $CH_3NH_3PbI_{3-x}(SCN)_x$ perovskite based planar solar cells. *Chem. Commun.* **2015**, *51*, 11997–11999. [CrossRef] [PubMed]
25. Ke, W.; Xiao, C.; Wang, C.; Saparov, B.; Duan, H.S.; Zhao, D.; Xiao, Z.; Schulz, P.; Harvey, S.P.; Liao, W.; et al. Employing Lead Thiocyanate Additive to Reduce the Hysteresis and Boost the Fill Factor of Planar Perovskite Solar Cells. *Adv. Mater.* **2016**, *28*, 5214–5221. [CrossRef] [PubMed]
26. Nanu, M.; Schoonman, J.; Goossens, A. Nanocomposite three-dimensional solar cells obtained by chemical spray deposition. *Nano Lett.* **2005**, *5*, 1716–1719. [CrossRef]

27. Cui, X.; Chen, Y.; Zhang, M.; Harn, Y.W.; Qi, J.B.; Gao, L.K.; Lin, Z.W.; Huang, J.S.; Yang, Y.K.; Lin, Z.Q. Tailoring carrier dynamics in perovskite solar cells via precise dimension and architecture control and interfacial positioning of plasmonic nanoparticles. *Energy Environ. Sci.* **2020**, *13*, 1743–1752. [CrossRef]
28. Chen, J.; Zuo, L.; Zhang, Y.; Lian, X.; Fu, W.; Yan, J.; Li, J.; Wu, G.; Li, C.Z.; Chen, H. High-Performance Thickness Insensitive Perovskite Solar Cells with Enhanced Moisture Stability. *Adv. Energy Mater.* **2018**, *8*, 1800438. [CrossRef]
29. Zhang, B.; Zhang, M.J.; Pang, S.P.; Huang, C.S.; Zhou, Z.M.; Wang, D.; Wang, N.; Cui, G.L. Carrier Transport in $CH_3NH_3PbI_3$ Films with Different Thickness for Perovskite Solar Cells. *Adv. Mater. Interfaces* **2016**, *3*, 1600327. [CrossRef]

Disclaimer/Publisher's Note: The statements, opinions and data contained in all publications are solely those of the individual author(s) and contributor(s) and not of MDPI and/or the editor(s). MDPI and/or the editor(s) disclaim responsibility for any injury to people or property resulting from any ideas, methods, instructions or products referred to in the content.